3rd International Conference on Emerging Trends in Engineering, Technology, Science and Management
(IETE) Institution of Electronics and Telecommunication Engineers, New Delhi, India
11th June 2017, www.conferenceworld.in
(ICETETSM-17)
ISBN: 978-93-86171-48-1

Study on Photoluminescence of Europium Oxide Nanoparticles

Rachna Ahlawat

Materials Science Lab, Department of Physics, Ch. Devi Lal University, Sirsa, Haryana (India)

ABSTRACT

The optical properties of Eu_2O_3 nanoparticles dispersed in SiO_2 powder sample were investigated using photoluminescence (PL) spectroscopy as well as absorption spectroscopy as a function of temperature. In absorption spectra, the band edge absorption was observed at 305 nm having red shift with temperature due to well known quantum size effect. The luminescent enhancement is attributed to efficient resonant excitation of the Eu^{3+} luminescent and subsequent emission from $^5D_0$ ^7F_J states due to Eu^{3+} centers being embedded in low site symmetry positions which make the radiative transition largely allowed. However at much higher temperature, the prominent peak (~ 614 nm) is almost disappeared may be due to agglomeration/ temperature quenching. High excitation density allows interaction between excited centers and additional non-radiative pathway such as cross-relaxation results in lower luminescence quantum efficiency.

Keywords: Eu_2O_3 nanoparticles, XRD, Absorption spectra, Tauc's plot, PL etc.

I. INTRODUCTION

Solid luminescent materials have attracted much attention during the last decades, because of their wide range of applications in our daily life such as in lamps, sensors, X-ray detectors, and fluorescent tubes. One strong research focus is on the improvement of the quantum yields or the spectral energy distribution. With their narrow emission peaks, rare earth luminescent materials soon became important in this area. Recently, new fields of applications e.g., novel laser materials, luminescent markers in biological devices, or light-emitting diodes, and specially nano phosphors have been established and there still has been a lot of effort devoted to the further development of new lanthanide-doped oxides with improved chemical stability. For this goal, the lanthanide ions must be inserted into a stable inorganic, organic, or inorganic-organic hybrid matrix. Particularly, the incorporation of lanthanide ions into inorganic mesoporous hosts with high specific surface area has attracted much interest in recent. Silica (SiO_2) is an excellent host material for rare earth ions because of its high transparency, compositional variety and easy mass production. There are many reports on study of luminescent properties of different trivalent rare earths (e.g. Sm^{3+}, Ce^{3+}, Tb^{3+}, Er^{3+}, Yb^{3+}, Pr^{3+}) doped in silica along with different sensitizers to obtain strong emission [1-3]. The number of works reported on the luminescence of trivalent europium (Eu^{3+}) doped silica is limited [4]. All these reports suggest that rare earth alone cannot show luminescence in silica matrix unless any energy transferring activator is added. In this regard, it is important to examine the optical properties (absorption & emission spectra) of silica doped with Eu^{3+} ion only. Because such a glassy transparent luminescent matrix can have immense potential as a spectrum modifying layer for incoming solar radiation as well as antireflection property when integrated with a solar cell.

(ICETETSM-17)
ISBN: 978-93-86171-48-1

The effect of concentration on the absorption and luminescent properties of several rare earth ions incorporated into sol-gel silica have been reported by many researchers. But the effect of temperature study is still limited. Therefore, we have attempted to observe the effect of temperature on the absorption spectra, band gap energy and emission spectra of Eu^{3+} doped SiO_2 matrix. Interesting results are investigated due to evolution of crystalline phase of Eu_2O_3 and SiO_2 (quartz) at higher temperature.

II. EXPERIMENTAL

2.1 Sample Preparation

The preparation and structural properties of Eu^{3+}:SiO_2 nanopowder has earlier been discussed in the chapter 4, under section 4.2. The optical absorption spectra have been observed by using Lambda 750 (Perkin Elmer) UV-Vis-NIR spectrophotometer in 250-500 nm range. The photoluminescence (PL) properties of the synthesized samples were studied with fluorescence spectrophotometer F-7000 Hitachi having Xenon lamp as its excitation source (250-1600 nm). For the measurement of the absorption characteristics, 0.03 gram of the each synthesized Eu^{3+}:SiO_2 nanopowders were separately dispersed in DMSO to make a $0.01ML^{-1}$ solution and then separately they were taken in quartz cuvette for observations.

2.2 Characterizations

The x-ray diffractograms were taken with the help of XPERT-PRO x-ray diffractometer operated at 45 kV and 40 mA, using monochromatic Cu Kα radiation of wavelength 1.5406 Å in the different 2^o ranges. The optical absorption spectra have been observed by using Lambda 750 (Perkin Elmer) UV-Vis-NIR spectrophotometer in 200-900 nm range. For the measurement of the absorption characteristics, 0.03 gram of the each synthesized Eu_2O_3:SiO_2 nanopowders were dispersed in DMSO to make a $0.01ML^{-1}$ solution and then separately they were taken in quartz cuvette for observations. The photoluminescence (PL) properties of the synthesized samples were studied with F-7000 Hitachi fluorescence spectrophotometer having Xenon lamp as its excitation source (250-1600 nm).

III. RESULTS AND DISCUSSIONS

3.1 X-Ray Diffraction (XRD) Analysis:

XRD technology can be used for phase identification, structural analysis and grain size determination. X-ray diffraction studies were carried out to study the structural evolution of europium oxide nanoparticles dispersed in silica matrix. XRD pattern of the sample N3 annealed at 1000^oC has been shown in Fig. 3.1. The XRD pattern of this sample revealed that sudden heating at much higher temperature produces mixed crystalline phases of Eu_2O_3 and silica. During the synthesis of nanopowder we got different type of structure at different annealing temperatures. The XRD patterns for sample N1 and N2 are amorphous in nature therefore, are not presented here. The XRD pattern is selected only for 1000^oC, because at higher temperature T >1000°C, agglomeration of particles increases and conversion of oxides in rare earth silicates starts to form.

(ICETETSM-17)
ISBN: 978-93-86171-48-1

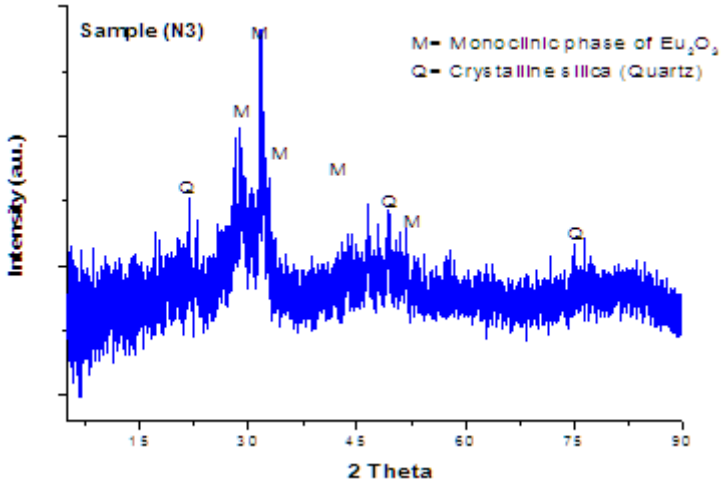

Figure 3.1: XRD pattern of sample N3 annealed at 1000°C.

In order to identify structure of the polycrystalline phase, plane corresponding to all major diffraction peaks at 2θ ~ 28.94°, 31.64°, 32.12°, 49.35° could be assigned to monoclinic phase of Eu_2O_3 by comparing the obtained data with the JCPDS card no. 34-0072 and space group C2/m. While some minor peaks at 2θ ~ 21.74°, 46.48°, 76.21°, corresponding to the crystalline silica (quartz) were also observed (JCPDS Card No.- 07-0346) [5-6]. In order to identify structure of the polycrystalline phase occurred in N3 sample, plane corresponding to diffraction peaks at 2θ ~ 28.94°, 31.64°, 32.12°, 49.35° could be assigned to Miller indices [111], [310], [112], [512] respectively which are well matched with the structural properties of Eu_2O_3:SiO_2 powder studied by other researcher [7]. We have calculated average crystalline size using well known Debye-Scherer's equation, {D=Kλ/βCos(θ)}, where θ is the Bragg angle of diffraction lines, λ is the wavelength of incident X-ray and β is the full width at half maximum (FWHM).

3.2 Optical Absorption Spectra

Absorption spectrum is used in order to study the optical behaviour of europium oxide nanopowder at room temperature. The UV-Vis absorption spectra of as prepared sample N1 and annealed samples N2, N3 are shown in the Fig. 3.2.

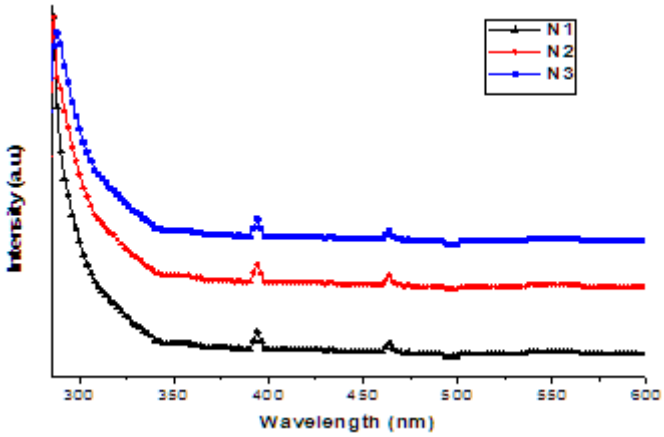

Figure 3.2: Absorption spectra of samples N1, N2 and N3.

(ICETETSM-17)
ISBN: 978-93-86171-48-1

Europium oxide doped SiO_2 nanopowder annealed at different temperatures yield similar emission spectra. The sample N1 has band edge absorption at 307 nm along with two small peaks at 394 and 465 nm. In sample N1, absorption at 305 nm could be attributed from excitation of silica lost or may be due to Eu-O charge transfer bond (CTB).

It is observed that two small peaks are corresponding to the absorption of Eu^{3+} 4f-4f transitions originated from the ground state $^7F_0$. These small peaks appeared at 394 and 465 nm could be assigned to the following transitions, respectively.

$^7F_0 \longrightarrow {}^5F_6$ and

$^7F_0 \longrightarrow {}^5D_2$

The peak intensity corresponding to Eu-O CTB is much higher than that of Eu^{3+} (f-f- absorption) indicating strong energy transfer from Eu-O CTB to Eu^{3+}. The peak intensity of Eu-O CTB increases with increasing of heat treatment temperature up to 1000°C. This is related to extent of reduction of non-radiative process for higher heat treatment samples. In annealed samples, N2 and N3 the band edge absorption peaks shifts towards the higher wavelength side at 320 nm & 330 nm, respectively, which is well matched with literature [7-8]. The observed shift in the absorption spectra has been occurred due to well known quantum confinement effect.

3.3 Calculation of Optical Band Gap Energy

The relation between the incident photon energy ($h\nu$) and the absorption coefficient (α) is given by the following equation:

$(\alpha h\nu)^{1/n} = A\,(h\nu - E_g)$

here A is a constant, α is absorption coefficient and E_g is the band gap energy of the material and the exponent *n* depends on the type of transition. For direct allowed transition n = 1/2, for indirect allowed transition n= 2, for direct forbidden n= 3/2 and for indirect forbidden n= 3. Direct band gap of the samples were calculated by plotting $(\alpha h\nu)^2$ verses hν and then extrapolating the straight portion of the curve on hν axis at α= 0 as shown in the Fig. 3.3.

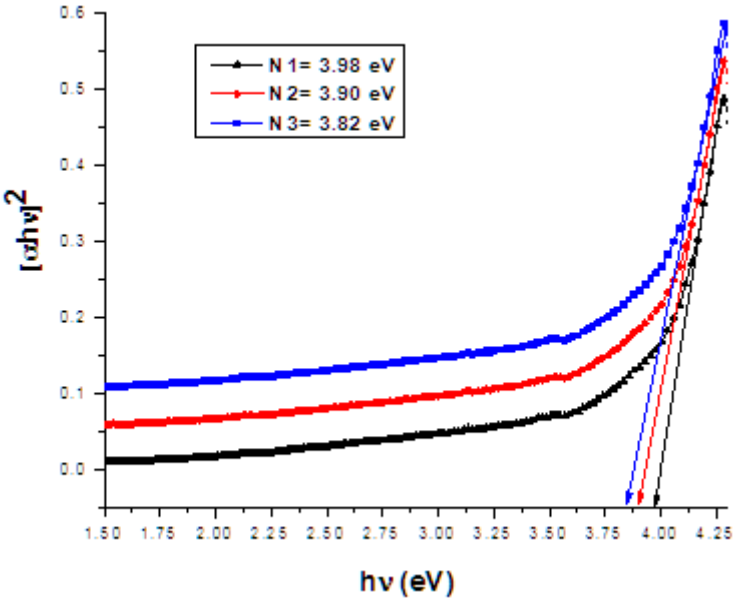

Figure 3.3: Tauc's Plot for samples N1, N2 and N3.

(ICETETSM-17)
ISBN: 978-93-86171-48-1

The band gap energy for the presented samples N1, N2 and N3 is calculated which is much smaller than the bulk Eu^{3+}-SiO_2 composite powder. The Tauc's Plots for direct transitions are shown in the Fig. 3.3. The extrapolations of the linear portions of these plots to $(\alpha h\nu)^{1/2} = 0$ give optical band gaps which are mentioned in table 3.1 along with cut off wavelength for all the prepared samples. In addition to this, the theoretical optical band gap energy can be calculated using below equation for comparing results, i. e. $E = hc/\lambda = 1240\ eV/\lambda\ (nm)$, here, h, c and λ are Planck's constant, velocity of light and cut off wavelength, respectively. Cut off wavelength is corresponding to the observed band edge absorption in the present study.

Thus, it is observed from the Fig. 3.3 that the calculated band gap is shifted toward lower energy (red shift) side as the annealing temperature increased. This is because as the samples are annealed at higher temperature the crystallites begins to move and tends to agglomerate easily forming bigger particles. As a result, the band gaps of the nanoparticles decrease with increasing annealing temperature. These results of observed absorption spectra and band gap values are well matched with the available literature [7].

Table 1: Comparison of calculated band gap with theoretical values.

Sample	Cut off wavelength (nm)	Optical band gap (eV) Observed	Optical band gap (eV) Theoretical
N1 (as prepared)	305	3.98	4.06
N2 (at 500°C)	320	3.90	3.87
N3 (at 1000°C)	330	3.82	3.75

3.4 Emission Spectra of Eu_2O_3:SiO_2 Nanoparticles

Fig. 3.4 shows the room temperature photoluminescence emission spectrum for sample N1 (as prepared) and annealed samples N2 (500°C), N3 (1000°C). The excitation wavelength is fixed at 305 nm in the present study. The as-prepared sample N1 shows broad emission peaks at 560, 614 and 704 nm with weak intensities. It is observed that the obtained emission spectrum is typically composed of $^4F_6 \longrightarrow {}^4F_6$ with $^5D_0 \longrightarrow {}^7F_J$ (J= 0,1,2,3,4) emission lines of Eu^{3+} ion, dominated by red emission $^5D_0 \longrightarrow {}^7F_2$ (614 nm), $^5D_0 \longrightarrow {}^7F_3$ at (618 nm).

The other emission peaks located at 560 nm ($^5D_0 \longrightarrow {}^7F_0$), ($^5D_0 \longrightarrow {}^7F_4$) 704 nm are also clearly illustrated in Fig. 3.4. The detailed value of peak position and corresponding intensity for each transition line is provided in table 2.

Table 2: PL peak position and intensity for each transition line.

Observed transitions	Sample N1		Sample N2		Sample N3	
	Wavelength (nm)	Intensity (a.u.)	Wavelength (nm)	Intensity (a.u.)	Wavelength (nm)	Intensity (a.u.)
$^5D_0 \longrightarrow {}^7F_1$	560	23.52	554	21.14	550	25.43
$^5D_0 \longrightarrow {}^7F_2$	614	39.23	614	70.71	614	20.49
$^5D_0 \longrightarrow {}^7F_3$	618	37.11	618	60.06	Missing	---
$^5D_0 \longrightarrow {}^7F_4$	704	35.44	702	32.42	700	44.50

(ICETETSM-17)
ISBN: 978-93-86171-48-1

From table 2, it is interesting to note that for annealed sample N2, the highest intense sharp emission peaks occurred at 554 nm and 614 nm and which correspond to magnetic ($^5D \longrightarrow {}^7F_1$) and electric ($^5D_0 \longrightarrow {}^7F_2$) dipole allowed transitions of Eu^{3+} ion. Similar peak positions were also reported in literature by many researchers [8-9]. It is known that the surface states and unsaturated dangling play a critical role in determining the overall PL characteristics of nanostructures. In the sample N2, the strongest emission peak was obtained in red region (614 nm), which makes it suitable for using it as a down-conversion phosphor. As the electric dipole transition ($^5D_0 \longrightarrow {}^7F_2$) is strongly dependent upon the local symmetry environment compared to the ($^5D_0 \longrightarrow {}^7F_1$) magnetic dipole transition, the high value of the ratio of luminescence intensity ($^5D_0 \longrightarrow {}^7F_2$) / ($^5D_0 \longrightarrow {}^7F_1$) transition ~3.0 suggests that Eu^{3+} ion is located in a low symmetry site in amorphous silica matrix [10]. Therefore, the resonant excitation between various energy levels of Eu^{3+} ions leads to the efficient absorption of UV-blue light eliminating any need of an additional sensitizer in Eu_2O_3:SiO_2.

Upon further heating at much higher temperature (~1000^{o}C), the amorphous powder transformed into crystalline monoclinic phase of Eu_2O_3 and quartz. Therefore due to high temperature, the luminescence intensity reduces drastically for sample N3 because of change in local symmetry environment of Eu^{3+}. This can happen due to enhanced non-radiative charge transfer between Eu^{3+} ions in close proximity in Eu_2O_3. Apart from temperature quenching, high excitation density allows interactions between excited centers and additional non-radiative decay pathways such as cross-relaxation, also resulting in lower luminescence quantum efficiency [11]. Therefore, the PL from as prepared sample was found to be weak and inefficient for any practical application, where as the PL intensity from annealed sample N2 turn out to be much stronger (>2 times). Moreover, the PL intensity of other bands becomes small, which indicate that there is a remarkable decrease in unsatisfied chemical bonds in the final powder. The most intense line at ~614 nm corresponds to the hypersensitive transition between $^5D_0$ and $^7F_2$ level of the Eu^{3+} ions and will be relatively strong if the surrounding symmetry is low.

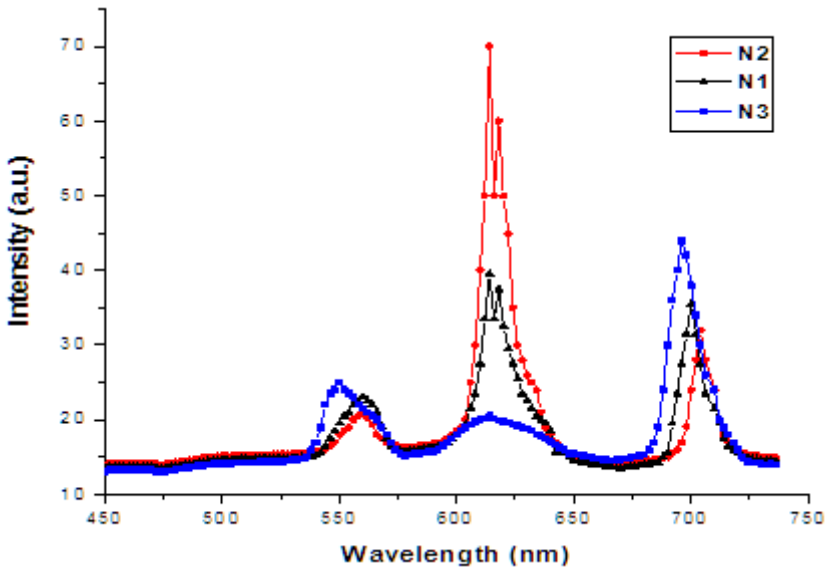

Figure 3.4: Emission spectra of samples N1, N2 and N3.

Therefore, temperature-dependent measurements show an increase of the emission intensity at low temperatures, because of the higher occupation probability of excited vibrational states with increasing temperature, resulting in an increase quenching process. Nevertheless, one may notice that in sample N3, the

(ICETETSM-17)
ISBN: 978-93-86171-48-1

relative intensity of transition like $^5D_0 \rightarrow {}^7F_1$ (560 nm) and $^5D_0 \rightarrow {}^7F_4$ (~700 nm) is not so much decreased and remains unaffected from temperature quenching. Also in sample N3, a sharp peak observed at ~618 nm is completely disappeared and intensity at 614 nm becomes negligible. The possible reason for this drastic change could be the observed crystallization of Eu_2O_3 and silica (quartz). Also some intrinsic impurities presented in the raw precursors of the vitreous matrix may produce such differences as observed by many researchers [12-13]. The significant luminescence band centered on 700 nm has also been reported in silicate, chalcogenide, tellurite and Er^{3+} doped TeO_2 glasses. The authors of these work claim that such a band is due to charged intrinsic defects in the glass network with deep energy levels, such as oxygen deficient centers in silicate glasses or dangling bonds in chalcogenide glasses.

IV. CONCLUSIONS

The XRD analysis proved that monoclinic structure of Eu_2O_3 was well grown along the crystalline phase of silica (quartz). The average sizes of the nanocrystallites were calculated from the diffraction line width based on the D–S formula is ~30 nm observed. In absorption spectra, the band edge absorption was observed at 305 nm having red shift with temperature due to well known quantum size effect. With increase in annealing temperature, band gap energy was also slightly increased.

In as prepared sample N1, successful immobilization of luminescent Eu^{3+} ions in amorphous silica matrix resulted in a bright red emitting luminescent material. In annealed sample N2, due to vaporization of water and organic residues, reduction of non-radiative transitions takes place which is responsible for the luminescent enhancement. The luminescent enhancement is attributed to efficient resonant excitation of the Eu^{3+} luminescent and subsequent emission from $^5D_0 \rightarrow {}^7F_J$ states due to Eu^{3+} centers being embedded in low site symmetry positions which make the radiative transition largely allowed. However at much higher temperature, the prominent peak (~ 614 nm) is almost disappeared may be due to agglomeration/temperature quenching. High excitation density allows interaction between excited centers and additional non-radiative pathway such as cross-relaxation results in lower luminescence quantum efficiency. Such studies have shown the PL emission band covering a large part of the visible spectra of the structurally disordered compound is very similar to that observed for nanocrystalline materials.

REFERENCES

[1] J. Mu, L. Liu, S. Kang, Nanoscale Res. Lett., 2 (2007) 100.

[2] Y. Hu, W. Zhuang, J. Hao, X. Huang, H. He, Open Journal of Inorganic Chemistry, 2 (2012) 6-11.

[3] M. Kubus, H. Meyer, L. Kienle, A. M. Klonkowski, J. Non-Crystt. Solids, 355 (2009) 1333.

[4] Y. Ding, H. Min, X. Yu, Mater. Lett., 58 (2004) 413.

[5] A. F. Khan, R. Yadav, S. Singh, V. Dutta, S. Chawla, Materials Research Bulletin, 45 (2010) 1562–1566.

[6] N. A. S. Omar, Y. W. Fen, K. A. Matori, S. H. A. Aziz, Z. N. Alassan, N. F. Samsudin, Procedia Chemistry 19 (2016) 21-29.

(ICETETSM-17)
ISBN: 978-93-86171-48-1

[7] T. G. V. M. Rao, A. R. Kumar, K. Neeraja, N. Veeraiah, M. R. Reddy, J. Alloys and Compounds, 557 (2013) 209-217.

[8] N. Zhang, R. Yi, L. Zhou, G. Gao, R. Shi, G. Qiu, X. Liu, Mater. Chem. Phys., 114 (2009) 160.

[9] L. R. Singh, R. S. Ningthoujam, V. Sudarsan, I. Srivastava, S. D. Singh, G. K. Dey, S. Kulshreshta, Nanotechnology, 19 (2008) 055201.

[10] A. F. Khan, R. Yadav, S. Singh, V. Dutta, S. Chawla, Materials Research Bulletin, 45 (2010) 1562–1566.

[11] S. Mochizuki, T. Nakanishi, K. Ishi, Appl. Phys. Lett., 79 (2001) 3785.

[12] V. K. Tikhomirov, A. B. Seddon, D. Furniss, M. Ferrari, J. Non-Cryst. Solids, 326 (2003) 296.

[13] S. A. Lourenco, N. O. Dantas, E. O. Serqueira, W. E. F. Ayta, A. A. Andrade, M. C. Fiiadelpho, J. A. Sampio, M. J. V. Bell, M. A. Pereira-da-Silva, J. of Luminescence, 131 (2011) 850-855.